Article

The Impact of Restricting Air Intake in Self-Aspirated Flotation Cells at Los Pelambres Concentrator

Michel Morales Gacitúa [1], Miguel Maldonado Saavedra [2,*] and Luis Vinnett [3,*]

[1] Superintendencia de Metalurgia, Minera Los Pelambres, Antofagasta Minerals, Salamanca 1950410, Chile; mmorales@pelambres.cl

[2] Departamento de Ingeniería Metalúrgica, Universidad de Santiago de Chile, Santiago 9170022, Chile

[3] Departmento de Ingeniería Química y Ambiental, Universidad Técnica Federico Santa María, Valparaíso 2390123, Chile

* Correspondence: miguel.maldonado.s@usach.cl (M.M.S.); luis.vinnett@usm.cl (L.V.)

Abstract: This article describes the impact of restricting the air intake in industrial 250 m^3 WEMCO flotation cells at Los Pelambres concentrator. The influence of air restriction on the hydrodynamic and metallurgical performance of this type of machine was evaluated. The experiments were conducted in single flotation cells and entire rougher banks. In all cases, the gas holdup was measured to estimate the effectiveness of the obstruction system to decrease the air concentration. In single cells, axial profiles for solid percentage and particle size were evaluated. In addition, mass balances were conducted to assess the copper recoveries and concentrate features. In individual cells, air restriction led to a decrease in the gas holdup. However, this slight change was enough to obtain a more stable froth zone and a better solid suspension. The latter was observed as: (i) a higher P80 below the pulp–froth interface, (ii) a less diluted pulp at this level, (iii) a slightly higher Cu recovery, and (iv) a coarser concentrate product. A mineralogical analysis of the concentrate sample also showed the presence of coarser liberated Cu-sulfide particles. The results in single cells suggested an improvement in the recovery of coarse particles via more intense solid suspension. The air intake was also restricted in three rougher banks to assess the impact of air obstruction on the overall performance of the respective circuit. Eleven out of fourteen cells were operated with air restriction, which led to a significant improvement in recovery of 0.9%–1.6% (absolute), at a 95% confidence level. Size-by-size mass balances were also conducted for the rougher circuits, which proved that the recovery improvements were justified by the simultaneous increase in the recovery of coarse and fine particles. Thus, a restriction in the air intake showed that a decrease in the gas holdup (and in the bubble surface area flux) was compensated by better solid suspension and a higher collision efficiency in the draft tube. The former promoted the recovery of coarse particles in the quiescent zone, whereas the latter improved the interaction between bubbles and fine particles. Further developments are being made to implement a regulatory control strategy for the air intake in self-aspirated flotation cells and to use this approach for optimizing industrial flotation banks.

Keywords: self-aspirated flotation cells; WEMCO cells; flotation banks; air restriction

1. Introduction

A flotation plant comprises multiple flotation stages, such as roughing, cleaning, and scavenging, to attain a targeted metallurgical performance. These stages consist of flotation units or banks with the latter typically composed of serial arrangements of mechanical cells, i.e., the tail of a cell is the feed to the subsequent cell down the bank. Mechanical cells can be of different types; for example, forced-air, self-aspirated, or reactor–separator cells. Regardless of the machine technology, the mineral slurry enters the first cell of the bank, where hydrophobic particles have the first chance to be attached to air bubbles. The particles that remain in the pulp are transported by gravity to the next cell, where the particles have another opportunity to attach to bubbles and be recovered. The process

is repeated down the bank until the particles are rejected into the overall tailings of the circuit. Due to its serial structure, the manner in which individual cells are operated to achieve optimal performance is not straightforward [1]. In addition, flotation performance is not measured cell-by-cell but only for the overall bank, which limits the application of serial-stage optimization techniques, such as dynamic programming [2–4].

Once the chemistry is adequately set, the flotation performance depends on modifying local variables such as the froth depth or gas rate in each cell to achieve targeted bank recoveries and concentrate grades. Previous studies on forced-air flotation machines have shown that the way in which air is distributed down the bank has a critical impact on the separation performance [5–8]. As air cannot be easily modified in self-aspirated machines, froth-depth profiling is commonly implemented to obtain targeted metallurgical indices [2,9,10]. Using theoretical analysis, Maldonado et al. [11] showed that a balanced cell-by-cell recovery profile maximizes the separation efficiency for a given targeted recovery. This theoretical analysis has been confirmed by simulation and extended to the case of the separation of a valuable mineral from entrained gangue, in which a balanced mass-pull profile provides the best results [12]. More recently, available data for continuous flotation banks have been reviewed, supporting the strategy of balanced mass-pull profiling for optimization purposes [13].

Most industrial optimization research in flotation has focused on forced-air machines [5–8]. In self-aspirated WEMCO cells, the movement of a paddle–wheel-type impeller in the upper part of the cell induces a vortex that extends to the standpipe and draws exterior ambient air into the rotor, which is dispersed in the form of small bubbles. At the same time, the rotor is partially immersed into a pipe (draft tube) that extends to the false bottom of the cell. A lower vortex is induced in the draft tube that draws slurry from the bottom of the cell up to the rotor, where the particles and bubbles collide. The air intake and pulp circulation are then interrelated [14]. For example, as the rotor speed increases, stronger upper and lower vortices are generated; consequently, aspirated air and slurry circulation increase. The submergence of the rotor also increases the circulation of the slurry at the expense of reducing the air intake [14].

Air restriction has not received enough attention to control self-aspirated cells. There are two causes for limited research on this topic: (i) lower gas holdups typically imply lower bubble surface area fluxes, and thus, lower collection zone recoveries are expected; (ii) the default suction system is believed to operate close to an optimum condition. Even though air restriction results in a reduced contact area between bubbles and particles, the multivariable nature of flotation plays a critical role in the overall efficiency of the process. In forced-air mechanical cells, an excess of air in the impeller zone at a constant agitation speed leads to erratic solid suspensions [15–17]. As the impeller has a fixed volumetric capacity, the lower (local) effective volume caused by the presence of air reduces the volume of pulp that can be circulated [15]. As suggested by intensified flotation technologies [18], promoting the slurry to circulate through the impeller systems favors particle–bubble interactions, which is critical for improving the recovery of fine particles. The increase in pulp circulation also favors the suspension of coarse particles and potentially their recovery. In self-aspirated cells, Yianatos et al. [19] proved via radioactive tracing that the pulp only passes five times through the impeller before leaving the machine. Therefore, any increase in pulp circulation results in more chances to collect difficult-to-float particles. To date, most of the studies on suspensions in flotation machines have been based on extreme comparisons in terms of aeration: aerated versus unaerated slurry suspensions [17,20,21]. These studies have only been oriented to analyze hydrodynamic machine features without evaluating the potential metallurgical improvement in self-aspirated machines under air restrictions.

This study shows that as the air intake is restricted, pulp circulation increases, which favors the suspension of coarse particles and, therefore, their recovery. The impact of restricting the air injection in 250 m^3 WEMCO cells at Los Pelambres concentrator was assessed. Although the self-aspirated cells at Los Pelambres are equipped with a damper-type valve in the air intake pipe, operators do not use it as a control variable. However, restrict-

ing the air intake had a significant impact on increasing the turbulence in the flotation cells and has consistently been observed in the operation of the rougher flotation circuit.

2. Materials and Methods

2.1. Flotation Circuit Configuration at Los Pelambres

Figure 1 shows a diagram of the rougher flotation circuit at Los Pelambres concentrator consisting of eight parallel flotation banks. Flotation banks E to H comprise nine 127 m³ self-aerated WEMCO cells arranged in a 1-2-2-2-2 configuration. The other flotation banks (A to D) consist of 250 m³ WEMCO cells. Banks C and D are arranged in a 1-1-1-1-1-1 (6 cells) configuration, whereas banks A and B are arranged in a 1-1-1-1-1 (5 cells) configuration. The dashed red line in Figure 1 represents an optional configuration for the distributor box of SAG line 3, which allows a fraction of the pulp to be fed to the rougher bank C. This study focused on the rougher banks comprising 250 m³ WEMCO cells. Hydrodynamic and metallurgical characterizations of single cells and overall banks (banks A, C, and D in Figure 1) were conducted, restricting the air intake in self-aspirated cells. The non-restricted condition was used as a reference for comparison purposes. In all comparisons, the same froth depths were kept in the machines or circuits under study.
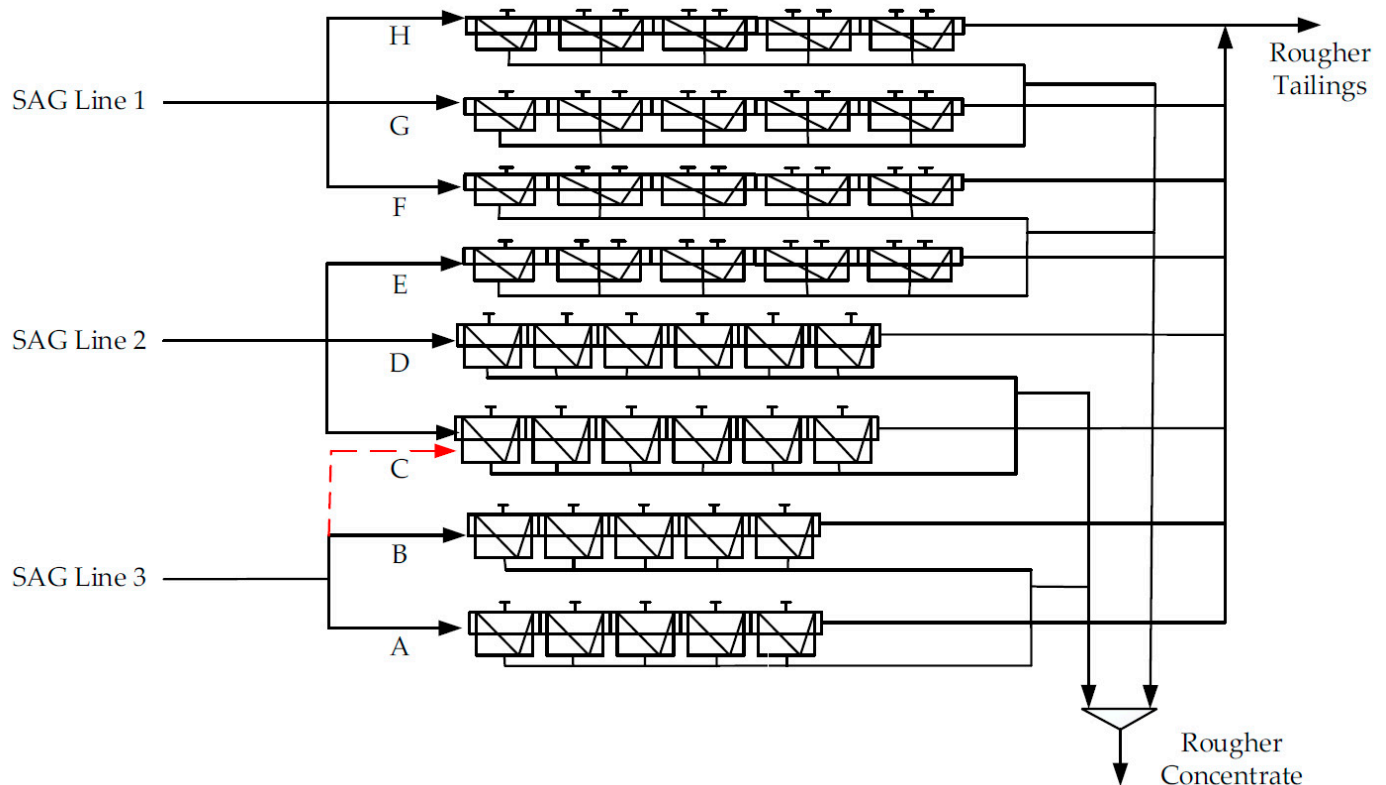

Figure 1. Rougher flotation circuit at Minera Los Pelambres [22].

Figure 2a schematizes the main components of a 250 m³ self-aspirated WEMCO cell at Los Pelambres. Figure 2b shows a metallic cap with a ball valve installed on top of the air intake pipe to restrict the injection of air. This setup was effective at modifying the gas holdup in the cell. Although this obstruction of air allowed the air intake to be changed, the air flowrate was not regulated. Two individual cells were characterized according to their operational availability: (i) the second cell of bank A and (ii) the sixth cell of bank C.
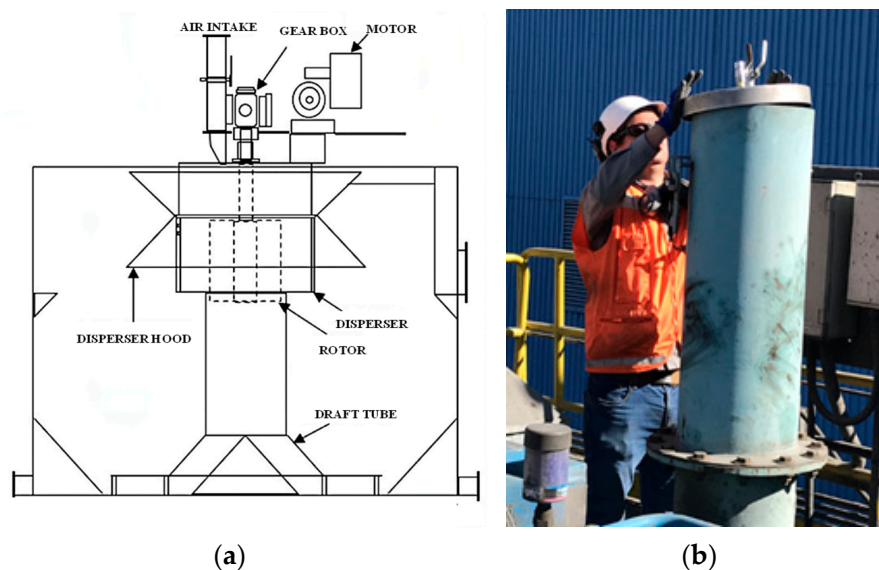
(a)　　　　　　　　　　　　　　　　**(b)**

Figure 2. (**a**) WEMCO cell schematic; (**b**) a restriction of the air intake by installing a metallic cap with a ball valve.

2.2. Gas Holdup Measurements

The gas holdup was measured using the JK Tech Air Holdup Probe [23]. This sampler allowed one liter of aerated slurry to be captured. The sample was then poured into a graduated beaker to calculate the volume of the unaerated slurry. The gas holdup was determined from the difference between the sampler volume and that of the unaerated slurry. For each experimental condition, an average of four holdup measurements was obtained. The gas holdup was estimated when characterizing single cells and overall rougher banks under restricted and non-restricted air intakes.

2.3. Axial Solid Profiles

To characterize the solid suspension in single cells, pulp samples were collected at different cell depths. These samples were taken at a 70% radial distance. The samples were analyzed in terms of their solid percentage and particle size distribution. These measurements allowed the characteristics of solid suspensions to be determined with and without air restrictions.

2.4. Metallurgical Assessment

Mass balances were conducted in the second cell of rougher bank A and in the overall rougher banks A, C, and D.

In single cells, the feed, concentrate, and tail streams were sampled. The dried samples were assayed to determine copper grades and recoveries. Molybdenum and iron grades were also measured, and data reconciliation was performed, taking advantage of information redundancy [24,25]. The metallurgical indices were compared when activating or deactivating the air restriction. The concentrates were also analyzed using QEMSCAN (Quantitative Evaluation of Minerals by Scanning Electron Microscopy) to determine the impact of limiting the air inlet on the mineralogy and liberation patterns of these samples.

When characterizing the rougher banks, the recoveries registered from the Distributed Control System (DCS) were studied over a period of two months. During one week of this period, 11 cells of the rougher banks A, C, and D were operated with air restriction. The comparison of Cu recoveries with and without air restrictions allowed for the impact of limiting the air intake on metallurgical performance to be determined. In addition, mass balances were conducted for banks A, C, and D to determine size-by-size recoveries. This non-restricted condition was again compared to that with 11 cells operated with air restriction. The feed, concentrate, and tailings of the rougher banks were sampled.

Concentrates of rougher banks C and D shared the same launder, as shown in Figure 1. The recoveries of these banks were then analyzed as a combined rougher stage. The dried samples were screened, and the finest classes were additionally classified via Cyclosizing. The screened samples were then assayed for Cu to obtain the respective size-by-size recoveries. These recoveries were compared, considering the non-restricted air condition (baseline) and two different air-restricted conditions.

3. Results and Discussion

3.1. Single Cells Assessment

This section describes the impact of restricting the air intake on the machine hydrodynamics and metallurgical performance of single WEMCO cells.

3.1.1. Hydrodynamic Conditions in Single Flotation Cells

Figure 3 shows top-of-the-froth images obtained when the second cell of bank A was operated with no air restriction (baseline, Figure 3a) and under air restriction (Figure 3b). A gas holdup reduction from 12% to 8% was observed from this change. The froth texture changed, leading to more stable and loaded froths for the air-restricted case. A preliminary observation showed the potential to modify the metallurgical performance in single self-aspirated cells when restricting the air intake.
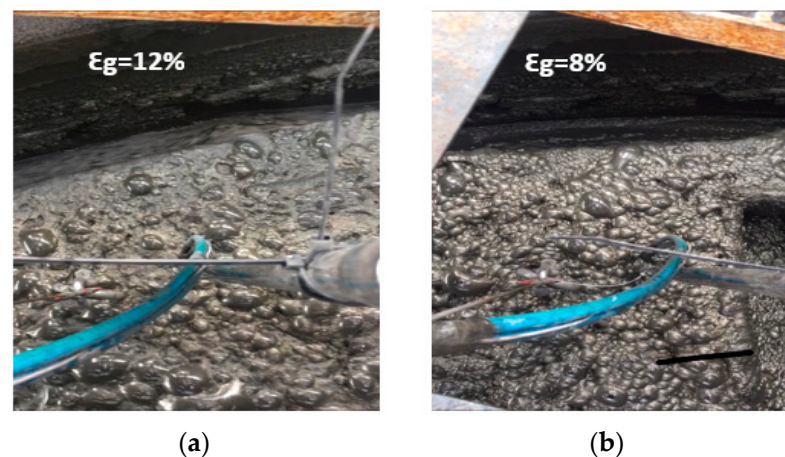

(**a**)   (**b**)

Figure 3. Top-of-the-froth images: (**a**) Unrestricted air intake, (**b**) Restricted air intake.

Concentrate samples were analyzed for solid concentration and particle size. Table 1 summarizes the results in the second cell of bank A, in which particle size was quantified in terms of the P80. Significant increases in the solid concentration and particle size were observed for the concentrate samples, when this cell was operated under an air-restricted condition. A reduction in water recovery followed by an increase in the solid concentration was expected when air intake was restricted and as gas holdup decreased. However, there was a significant increase in the P80. The decrease in air intake was hypothesized to improve pulp circulation, which agrees with the results reported in the literature [15–17] for forced-air machines. The increase in pulp circulation improved the suspension of coarse particles, thus promoting their recovery.

Table 1. Solid percentage, particle size, and gas holdup in the second cell of bank A, under non- and air-restricted conditions.

	Gas Holdup			
	12% (Non-Resctricted)		8% (Air Restricted)	
	Solids (% w/w)	P80 (μm)	Solids (% w/w)	P80 (μm)
Concentrate	11.4	<38	48.4	61.7

　　　　To further investigate these findings, pulp samples were taken at a 70% radial distance and at different depths inside the cell. These samples were analyzed for solid concentration and particle size. Figure 4 shows the axial profiles for the solid percentage and particle size in the nominal and restricted-air conditions. In the former, a diluted zone underneath the pulp–froth interface was observed (dashed, blue line), exhibiting approximately 23% of solids and P80 ≈ 100 μm. When the air intake was restricted, the upper part of the cell experienced an increase in both the solid concentration (~39% w/w) and P80 (~170 μm).
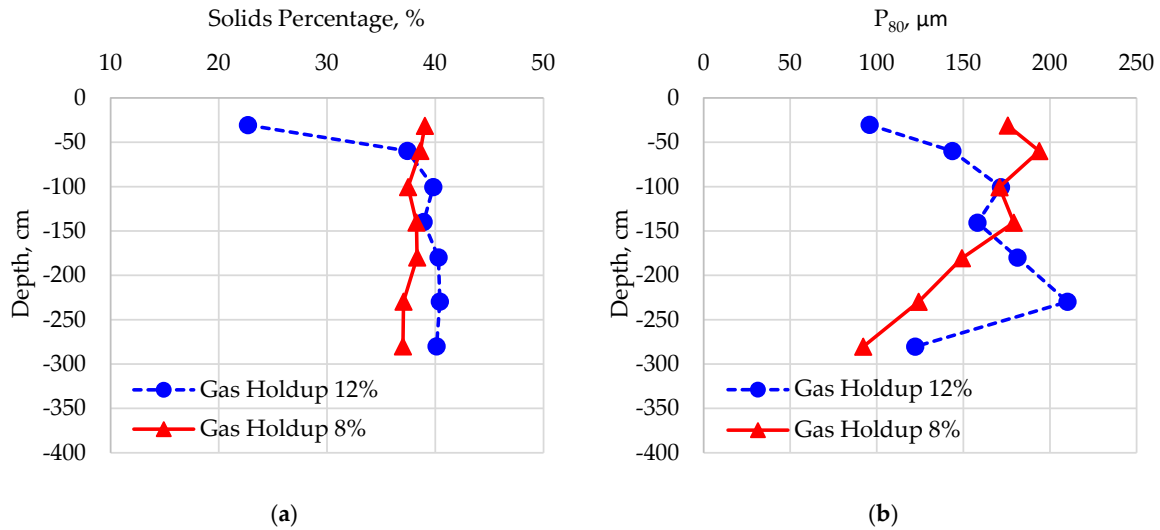

Figure 4. Axial profiles in the second cell of bank A: (**a**) Solid percentage, (**b**) Particle size.

　　　　To better visualize the impact of restricting the air intake on solid suspension in the WEMCO cell, the classification function proposed by Zheng et al. [26] was determined for the nominal and air-restricted conditions. This function is calculated from solid-to-water mass ratios, w_i, in a specific size class i, by dividing the w_i values measured below the pulp–froth interface by the w_i values measured in the tailings. A flat classification curve implies no segregation, whereas a flat profile approaching 100% implies no segregation nor dilution. Pulp samples were then drawn from underneath the froth and tailings of the sixth cell of bank C. For the unrestricted air condition, a gas holdup of 12% was measured, which was reduced to 7% when the suction pipe was obstructed. Figure 5 compares the classification functions. Mixing was significantly improved over a wide range of particle sizes when restricting the air intake.
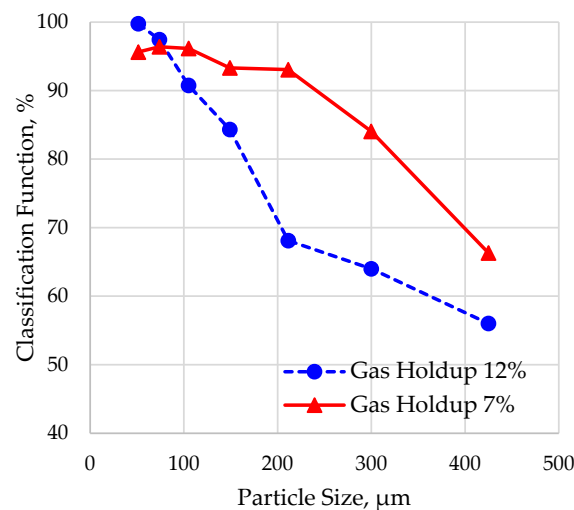

Figure 5. Classification function in the sixth cell of bank C for nominal (ε_G = 12%) and air-restricted (ε_G = 7%) conditions.

3.1.2. Metallurgical Performance in Single Flotation Cells

A significant change in WEMCO cell hydrodynamics was observed when air intake was restricted. The impact of these changes on the metallurgical performance of a single cell was evaluated. Pulp samples of the feed, concentrate, and tailings of the second cell of bank A were taken and analyzed for the solid concentration, particle size, and Cu, Mo and Fe grades. Table 2 summarizes the Cu results. The solid concentration and particle size of the concentrate samples increased once again for the air-restricted case. Table 2 also shows an increase of 1.4% for the Cu recovery when restricting the air compared to the baseline. This increase in recovery should be taken with some skepticism. The calculation of recovery using the two-product expression becomes sensitive to error propagation for cases where the separation is poor, as is usually the case for single cells [24,25]. An estimation of water recovery revealed a reduction from 6.6% to 2.1% when changing the operation from non-restricted to air-restricted. This result implies a decrease in entrained particles, which was confirmed by conducting a mineral composition analysis to the concentrate samples. Figure 6 shows a drastic reduction of more than 50% in the content of insoluble minerals, which justified an increase in the Cu concentrate grade (Table 2). Although there are uncertainties in the estimated Cu recoveries, the QEMSCAN analysis of the concentrate samples revealed the presence of liberated coarse particles when the cell was air-restricted (Figure 7b). These particles were not observed for the non-restricted case, as shown in Figure 7a.

Table 2. Metallurgical results in the second cell of bank A under non- and air-restricted conditions.

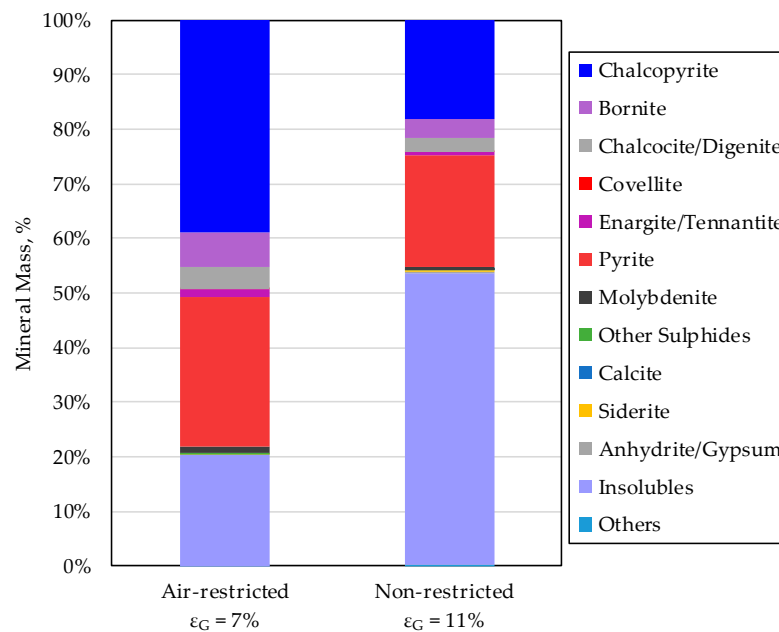| | Gas Holdup, % | | | | | |
| | 11.0% | | | 7.0% | | |
	Solids, %	P80, μm	Cu Grade %	Solids, %	P80, μm	Cu Grade %
Feed	33.2	125	0.11	33.8	130	0.11
Concentrate	11.4	38	2.41	22.5	115	3.54
Tailings	33.8	128	0.070	32.2	138	0.068
Cu Rec. %		37.5			38.9	

Figure 6. Mineralogical analysis for the concentrate samples in the second cell of bank A under non- and air-restricted conditions.
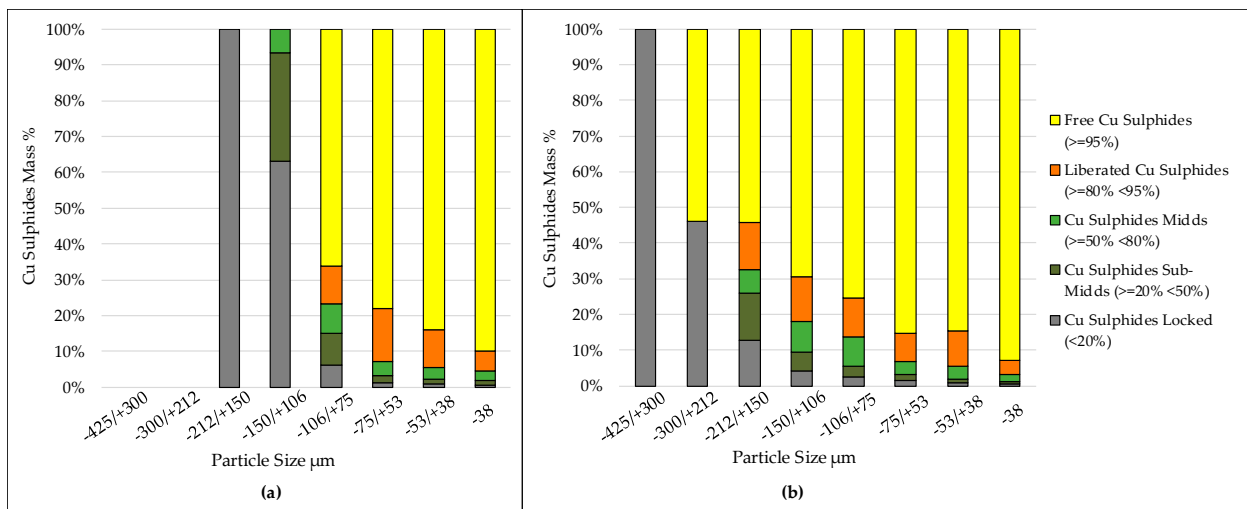
Figure 7. Liberation analysis for the concentrate samples in the second cell of bank A: (**a**) Non-restricted condition; (**b**) Air-restricted condition.

3.2. Circuit Assessment

This section describes the impact of restricting the air intake on the metallurgical performance of the rougher flotation circuit.

3.2.1. Overall Rougher Stage Performance

A sampling campaign was undertaken to quantify the metallurgical impact of restricting air intake in multiple cells of the rougher circuit. Gas holdup measurements were again conducted for the unrestricted air condition (baseline), as shown in Figure 8a, and also for the restricted case (Figure 8b). The entire bank B, the first cell of bank D, and the fourth and sixth cells of bank C were out of service and are labeled as O/S in Figure 8. From Figure 8b, the air intake was restricted in eleven out of fourteen cells, as highlighted by a checkmark. The average gas holdup reduction was almost −1.6% (absolute), only considering the manipulated cells. Air restriction was extended uninterruptedly for one week.
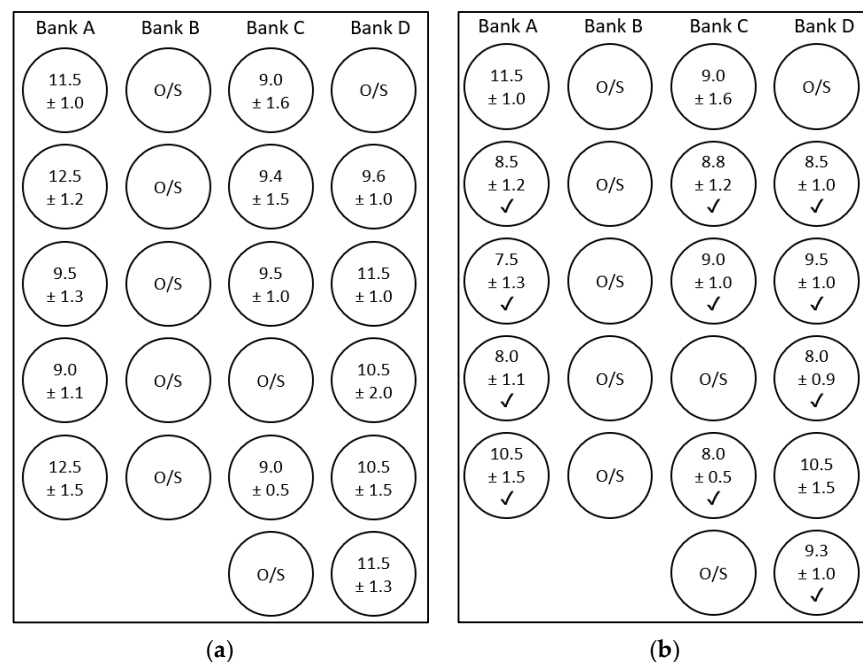

Figure 8. Gas holdup measurements (**a**) Before and (**b**) After restricting the air intake. O/S indicates out-of-service and the checkmarks in (**b**) indicate the cells subjected to air restriction.

From the metallurgical assessment of the rougher bank, Cu recoveries exhibited an increase from 91.1% to 92.3% when the cells were operated under restricted air intake. Figure 9 shows the time series of Cu recovery for the metallurgical assessment conducted over 2 months). The blue range highlights the period operated under the restriction strategy (Test On), as depicted in Figure 8b. The 95% confidence interval of the mean recovery difference (restricted minus non-restricted air) was 0.86%–1.62%, which implies that the observed differences were significant at α = 0.05. The 95% confidence intervals for the feed grades were 0.65%–0.76%, 0.58%–0.66%, and 0.63%–0.72% for the weeks before, during and after the restricted condition, respectively, indicating that an improvement in recovery was not attributed to significant changes in the mineralogy. It should be noted that the air flowrate was not automatically regulated in each cell, nor was a specific control strategy developed along the banks. Despite this, an increase in the rougher recovery was observed. This result suggests that the flotation performance can be improved by trading a reduction in the gas rate for an increase in the pulp circulation in WEMCO cells.
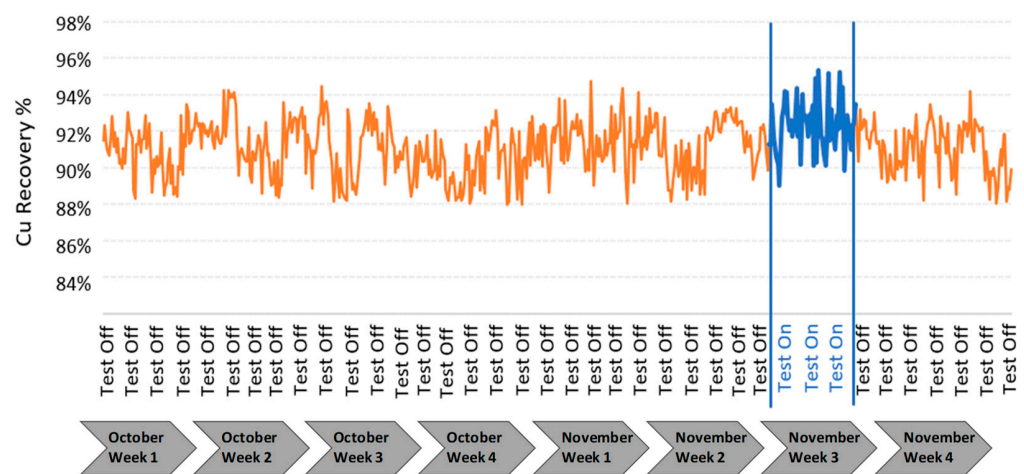

Figure 9. Cu recovery before, during and after restricting the air-intake, as described in Figure 8.

3.2.2. Size-by-Size Rougher Recoveries

Additional campaigns were conducted to determine size-by-size rougher recoveries for the conditions described in Figure 8. The non-restricted condition was replicated eight times to obtain a reference size-by-size recovery trend. In addition, the restriction scheme shown in Figure 8b was tested under two conditions. The valve openings employed for air obstruction were then manually modified to obtain two restriction levels. Banks C and D were assessed together as they shared a concentrate launder. Bank A was assessed individually, as bank B was out of service. The results for bank A are summarized in Appendix A. Table 3 presents the average gas holdups for banks C and D when they were operated under two air-restricted conditions. The non-restricted case is also presented as a reference. Figure 10 shows the size-by-size Cu recoveries for the two levels of air restriction (Test On) compared to the non-restricted case (Test Off, baseline). A moderate increase in the recovery of fine and coarse particles is observed with respect to the baseline; however, these differences were more significant when the average change in gas holdup was higher (Figure 10b). The same trend was observed in bank A, as shown in Figure A1 of Appendix A. Although the results in single flotation cells indicated an improvement in the suspension of coarse particles, the size-by-size results in the rougher circuit also showed an improvement in the recovery of fine particles, after decreasing air injection. Thus, a slight reduction in the level of aeration in self-aspirated cells led to an increase in the Cu recovery, as shown in Figure 9, which was justified by the simultaneous improvement in the recovery of fine and coarse particles.

Table 3. Average gas holdup in banks C and D for the two air-restricted conditions and the non-restricted case.

Average Gas Holdup for Banks C and D		
Non-Restricted	**Air-Restricted**	**Difference**
10.2%	9.5%	−0.7%
10.2%	8.8%	−1.4%

(**a**)

(**b**)
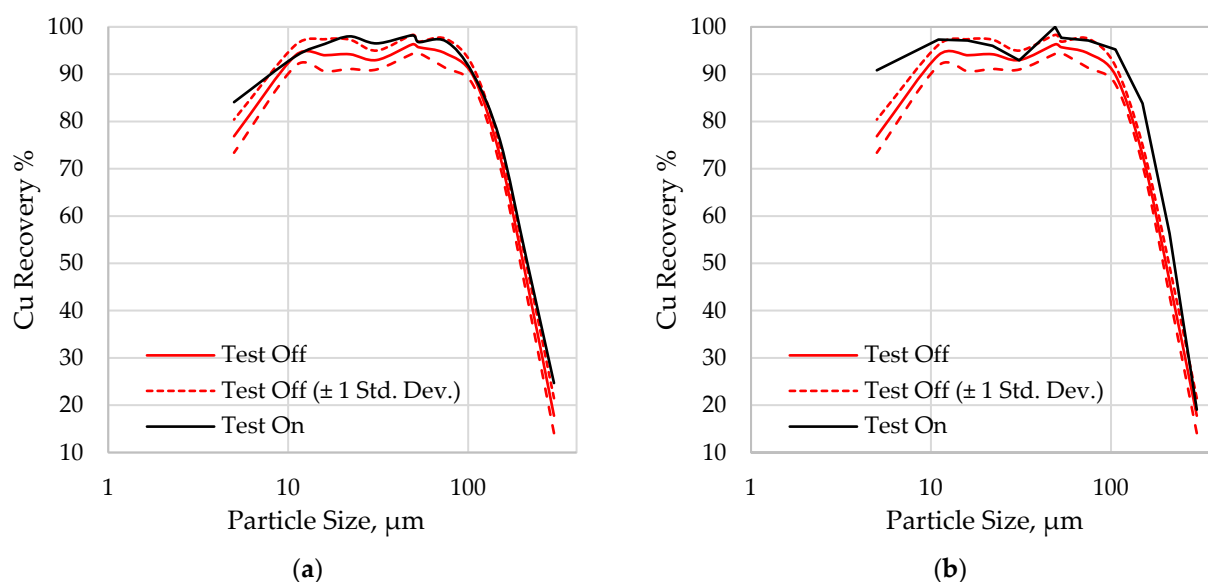
Figure 10. Size-by-size Cu recoveries in rougher banks C and D comparing the air-restricted case with the non-restricted case: (**a**) A low average air-restriction (a decrease of 0.7% in the average gas holdup with respect to the non-restricted case), (**b**) A moderate average air-restriction (a decrease of 1.4% in the average gas holdup with respect to the non-restricted case).

Results from Figures 4–10 show the potential of optimizing the air intake in self-aspirated cells to recover coarse particles. This finding agrees with those observed in forced air machines, as reported in flotation literature [15–17]. However, the size-by-size results in the rougher circuit indicate that the recovery of fine particles is also improved by restricting the air aspiration. Two possible mechanisms may have caused this improvement: (i) a decrease in bubble size; and (ii) an increase in the collision efficiency. Although both hypotheses are feasible, a reduction in bubble size does not seem to be the main cause for the higher recovery in the finer classes because the decrease in holdup was only moderate when restricting the air. An improvement in the collisions between fine particles and bubbles seems more likely, as less air favored the pulp circulation through the impeller. In addition, as the separation of low-grade ores is typically not constrained by carrying capacity limitations, the improvement in pulp circulation through the impeller compensates for a lower bubble surface area flux.

Further developments are being made to determine the operating range for the air restriction, which consistently leads to improvements in metallurgical indexes of single cells. The potential of employing air restriction as a control variable in a regulatory control strategy is suggested as a research area to optimize existing flotation circuits consisting of self-aspirated cells.

4. Conclusions

This paper evaluated the hydrodynamic and metallurgical impact of restricting the air intake in self-aspirated flotation cells. Experiments were conducted at industrial scale, evaluating the performance of single cells and entire banks consisting of 250 m^3 WEMCO machines. The main findings are summarized as follows:

- A restriction in air intake was viable in industrial self-aspirated machines. A consistent decrease in the gas holdup was observed when this intake was restricted. The air inlet obstruction was not regulated, and further developments are suggested on this subject.
- The air restriction in single WEMCO cells led to a better suspension of coarse particles and less diluted pulp below the pulp–froth interface, which agrees with results reported in the literature for forced-air machines. This operational improvement increased the concentrate grade and slightly increased Cu recovery at Los Pelambres concentrator.
- The implementation of an air restriction strategy in a bank of cells proved to be feasible. By restricting the air intake in eleven out of fourteen cells and in three rougher banks, Cu recovery increased by 0.9%–1.6% at a 95% confidence level in this stage.

An increase in rougher bank recoveries was justified by an improvement in the separation of coarse and fine particles. The air restriction improved the suspension of coarse particles, increasing their presence in the quiescent zone. The air restriction also favored the interactions between bubbles and fine particles in the draft tube. Thus, the regulation of air intake has the potential to be used for control purposes. Further hydrodynamic and metallurgical characterizations (e.g., froth features, froth recoveries, bubble size, and bubble load measurements) will be conducted under air intake restrictions to better understand recovery improvements in self-aspirated flotation cells.

Adequate instrumentation and regulatory control loops are recommended for air intake in self-aspirated flotation cells, improving the flotation performance of existing circuits. These components are the foundations to develop and optimize arrangements of cells in series at industrial scale.

Appendix A

Table A1 presents the average gas holdup in bank A when operated under non- and air-restricted conditions. Figure A1 shows the size-by-size Cu recovery for the two levels of air restriction (Test On) compared to the non-restricted case (Test Off, baseline). The same size-by-size trends observed in rougher banks C and D were found in rougher bank A, confirming the potential to improve the recovery of coarse and fine particles by optimizing the air intake.

Table A1. Average gas holdup for bank A for two air-restricted conditions and the non-restricted case.

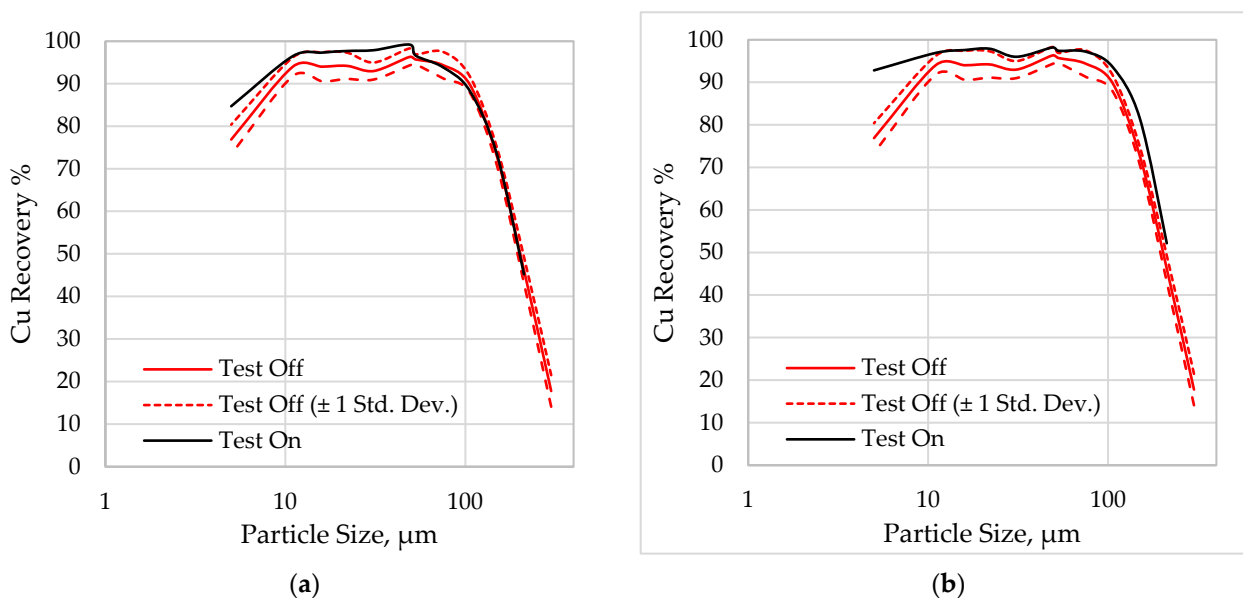| Average Gas Holdup for Banks C and D		
Non-Restricted	**Air-Restricted**	**Difference**
10.6%	9.4%	−1.2%
10.6%	8.7%	−1.9%

Figure A1. Size-by-size Cu recoveries in the rougher bank A, comparing the air-restricted case with the non-restricted scenario: (**a**) A low average air-restriction (a decrease in 1.2% in the average gas holdup with respect to the non-restricted case), (**b**) A moderate average air-restriction (a decrease in 1.9% in the average gas holdup with respect to the non-restricted case).

References

1.　Maldonado, M.; Araya, R.; Finch, J. An overview of optimizing strategies for flotation banks. *Minerals* **2012**, *2*, 258–271. [CrossRef]
2.　Maldonado, M.; Sbarbaro, D.; Lizama, E. Optimal control of a rougher flotation process based on dynamic programming. *Miner. Eng.* **2007**, *20*, 221–232. [CrossRef]
3.　Bellman, R. Dynamic programming. *Science* **1966**, *153*, 34–37. [CrossRef] [PubMed]
4.　Aris, R. *Discrete Dynamic Programming: An Introduction to the Optimization of Staged Processes*, 1st ed.; Blaisdell Publishing Company: New York, NY, USA, 1964.
5.　Gorain, B. Optimisation of flotation circuits with large flotation cells. In Proceedings of the Centenary of Flotation Symposium, Brisbane, QLD, Australia, 6–9 June 2005; pp. 843–851.
6.　Hadler, K.; Cilliers, J. The relationship between the peak in air recovery and flotation bank performance. *Miner. Eng.* **2009**, *22*, 451–455. [CrossRef]
7.　Cooper, M.; Scott, D.; Dahlke, R.; Finch, J.; Gomez, C. Impact of air distribution profile on banks in a Zn cleaning circuit. *CIM Bull.* **2004**, *97*, 1–6.
8.　Aslan, A.; Boz, H. Effect of air distribution profile on selectivity at zinc cleaner circuit. *Miner. Eng.* **2010**, *23*, 885–887. [CrossRef]
9.　Seguel, F.; Soto, I.; Krommenacker, N.; Maldonado, M.; Becerra Yoma, N. Optimizing flotation bank performance through froth depth profiling: Revisited. *Miner. Eng.* **2015**, *77*, 179–184. [CrossRef]
10.　Bergh, L.; Yianatos, J. Control of rougher flotation circuits aided by industrial simulator. *J. Process Control* **2013**, *23*, 140–147. [CrossRef]
11.　Maldonado, M.; Araya, R.; Finch, J. Optimizing flotation bank performance by recovery profiling. *Miner. Eng.* **2011**, *24*, 939–943. [CrossRef]
12.　Singh, N.; Finch, J. Bank profiling and separation efficiency. *Miner. Eng.* **2014**, *66*, 191–196. [CrossRef]
13.　Finch, J.A.; Tan, Y.H. Flotation bank profiling revisited. *Miner. Eng.* **2022**, *181*, 107506. [CrossRef]
14.　Degner, V.R. Recent WEMCO flotation technology advancements. *Resour. Process.* **1988**, *35*, 79–96. [CrossRef]
15.　Arbiter, N.; Harris, C.; Yap, R. The air flow number in flotation machine scale-up. *Int. J. Miner. Process.* **1976**, *3*, 257–280. [CrossRef]
16.　Lima, O.A.d.; Deglon, D.A.; Leal Filho, L.d.S. A comparison of the critical impeller speed for solids suspension in a bench-scale and a pilot-scale mechanical flotation cell. *Miner. Eng.* **2009**, *22*, 1147–1153. [CrossRef]
17.　Van der Westhuizen, A.; Deglon, D. Evaluation of solids suspension in a pilot-scale mechanical flotation cell: The critical impeller speed. *Miner. Eng.* **2007**, *20*, 233–240. [CrossRef]
18.　Hassanzadeh, A.; Safari, M.; Khoshdast, H.; Güner, M.K.; Hoang, D.H.; Sambrook, T.; Kowalczuk, P.B. Introducing key advantages of intensified flotation cells over conventionally used mechanical and column cells. *Physicochem. Probl. Miner. Process.* **2022**, *58*, 155101. [CrossRef]
19.　Yianatos, J.B.; Larenas, J.M.; Moys, M.H.; Diaz, F.J. Short time mixing response in a big flotation cell. *Int. J. Miner. Process.* **2008**, *89*, 1–8. [CrossRef]

20.　Schwarz, M.P.; Koh, P.T.L.; Wu, J.; Nguyen, B.; Zhu, Y. Modelling and measurement of multi-phase hydrodynamics in the Outotec flotation cell. *Miner. Eng.* **2019**, *144*, 106033. [CrossRef]

21.　Schwarz, M.; Koh, P.; Yang, W.; Nguyen, B. Investigation of the gas-liquid-particle multi-phase hydrodynamics of Wemco flotation cells. *Miner. Eng.* **2022**, *179*, 107388. [CrossRef]

22.　Henríquez, F.; Maldonado, L.; Yianatos, J.; Vallejos, P.; Díaz, F.; Vinnett, L. The Use of Radioactive Tracers to Detect and Correct Feed Flowrate Imbalances in Parallel Flotation Banks. *J* **2022**, *5*, 287–297. [CrossRef]

23.　Schwarz, S.; Alexander, D. Gas dispersion measurements in industrial flotation cells. *Miner. Eng.* **2006**, *19*, 554–560. [CrossRef]

24.　Wills, B.A.; Finch, J. *Wills' Mineral Processing Technology: An Introduction to the Practical Aspects of Ore Treatment and Mineral Recovery*; Butterworth-Heinemann: Oxford, UK; Waltham, MA, USA, 2015.

25.　Vinnett, L.; Yianatos, J.; Flores, S. On the mineral recovery estimation in Cu/Mo flotation plants. *Miner. Metall. Process.* **2016**, *33*, 97–106. [CrossRef]

26.　Zheng, X.; Franzidis, J.-P.; Johnson, N.; Manlapig, E. Modelling of entrainment in industrial flotation cells: The effect of solids suspension. *Miner. Eng.* **2005**, *18*, 51–58. [CrossRef]